Angle-of-Attack Convergence and Windward-Meridian Rotation Rate of Rolling Re-Entry Vehicles

DANIEL H. PLATUS*
The Aerospace Corporation, El Segundo, Calif.

A simple expression is derived for the influence of roll acceleration on the angle-of-attack convergence of rolling re-entry vehicles with pitch or yaw damping. Also included is an analysis of the windward meridian rotation rate of the rolling vehicle, which is coupled through the gyroscopic equations of motion to the angle of attack and roll rate. It is found that two modes of motion exist for which the windward meridian may be either oscillatory or rotary (i.e., the vehicle either oscillates about its roll axis relative to the wind or rotates continuously in one direction). The mode of motion depends on the initial re-entry conditions, and it is shown that a roll-induced instability can occur whereby the motion changes from one mode to the other, more stable mode. The analytical approximations are compared with computer solutions of the complete equations of motion.

Nomenclature

a = constant in phase plane analysis, $(\omega^2 + p_r^2)^{1/2}$
b = $Huv/4q \sin\gamma$ in angle-of-attack solution; constant in phase plane analysis, $(\frac{2}{3})\mu(\dot{p} + \nu p)$
c = constant in phase plane analysis, $\frac{1}{2}(\nu^2 - 2\dot{\nu})$
C_l = aerodynamic roll moment coefficient
$C_{N_\alpha}, C_{N_\beta}$ = aerodynamic normal force derivatives
C_{m_q} = aerodynamic pitch damping derivative
d = aerodynamic reference diameter; constant in phase plane analysis, $\mu p(\nu^2 - \dot{\nu}) \div (\nu^2 - 2\dot{\nu})$
H = reference altitude for exponential atmosphere
I = pitch or yaw moment of inertia
I_x = roll moment of inertia
l = static margin (distance of center of pressure aft of center of mass)
m = vehicle mass
M_ξ = aerodynamic roll moment
M_η = aerodynamic pitch moment
M_ζ = aerodynamic yaw moment
p = roll rate
p_r = reduced roll rate, $\mu p/2$
q = dynamic pressure
S = aerodynamic reference area
u = vehicle velocity
v = $\dot{y}$ in phase plane analysis
y = $\dot{\psi} - p_r$ in phase plane analysis
α = exoatmospheric precession cone half-angle
γ = path angle
ζ = yaw axis
ϵ = $-cd/2a^2$ in phase plane analysis
η = pitch axis
θ = total angle of attack (Euler angle)
κ = roll moment coefficient, $C_l qSd/I_x$
μ = inertia ratio, I_x/I
ν = pitch damping coefficient, $(qSd^2/2Iu)(-C_{m_q} + 2C_{N_\alpha} I/md^2)$
ξ = roll axis
ρ = atmospheric density
σ = ω/p_r
ϕ = roll orientation relative to wind (Euler angle)
ψ = precession angle (Euler angle)
ω = natural pitch frequency
Ω = exoatmospheric coning rate

Subscripts

ζ = yaw
η = pitch
ξ = roll
$+$ = oscillatory component

Superscripts

$(\dot{})$ = time derivative
$(\bar{})$ = quasi-steady component

Presented as Paper 69-100 at the AIAA 7th Aerospace Sciences Meeting, New York, January 22–22, 1969; submitted January 15, 1969; revision received October 15, 1969. This work was supported by the United States Air Force under Contract F04201-68-C-0200. The author is grateful to J. S. Whittier of The Aerospace Corporation Aerodynamics and Propulsion Research Laboratory for suggesting the phase plane approach to the stability problem. He is also grateful to Parviz Ghaffari, of the Aerospace Mathematics and Computation Center, and to J. Lesser for carrying out the numerical computations.

* Member Technical Staff, Mechanics Research Department. Member AIAA.

I. Introduction

OF particular interest in the performance evaluation of a re-entry vehicle is its angle-of-attack behavior during re-entry through the atmosphere. Understanding of the angle-of-attack behavior is essential for prediction of the vehicle's trajectory and for assessment of the thermal requirements of the vehicle's heat-protective system. In addition to the angle-of-attack behavior, a knowledge of the windward-meridian rotation rate is required if one is to couple the heating or ablation rate prediction with the vehicle dynamic motion.

The angle-of-attack convergence behavior of rolling re-entry vehicles has been studied, and a number of papers on the subject are reported in the literature.[1–5] All of these, however, treat the case of constant roll rate; only one includes the effect of pitch or yaw damping on the convergence envelope,[1] and none discusses in any detail the influence of exoatmospheric conditions on the subsequent angle-of-attack convergence and vehicle motion. Similar studies on the angle-of-attack behavior of spinning ordnance projectiles have also been made.[6] Because of the susceptibility of high-performance re-entry vehicles to roll resonance and other phenomena that can cause significant roll rate excursions, it is of interest to assess the influence of roll acceleration on the angle-of-attack convergence and on the windward-meridian rotation behavior.

It is known that the motion of a rolling missile consists of a combination of two precessional modes, one of which is generally dominant, as with a spinning top or gyroscope.[7] The windward-meridian rotation rate is strongly influenced by which precession mode prevails, which, in turn, is influenced by the exoatmospheric condition for a re-entry vehicle. In this paper a criterion is derived for predicting which mode will prevail under a given set of conditions.

The windward-meridian rotation behavior is then described accordingly.

The present study treats the vehicle motion during the period in which, because of misalignment with the flight path during re-entry, the angle of attack is large relative to the trim angle of attack from mass or configurational asymmetries. The quasi-steady or mean value of the angle-of-attack oscillation envelope is obtained as a function of time (or altitude) during this period.

II. Equations of Motion

The vehicle motion is described in terms of the Euler angles ψ, ϕ, θ, which describe the position of a set of body-fixed axes x,y,z relative to nonrotating axes X,Y,Z that translate with the vehicle, as shown in Fig. 1. The axes ξ, η, ζ are axes of roll, pitch, and yaw, respectively, relative to the plane of total angle of attack. They precess about the velocity vector with angular rate $\dot{\psi}$. If the principal moments of inertia about the ξ, η, ζ axes are I_x, I, I, respectively, and the aerodynamic moments about these axes are M_ξ, M_η, M_ζ, the moment equations of motion in terms of the Euler angles may be written[8]

$$\begin{aligned} M_\xi &= I_x(dp/dt) \\ M_\eta &= I\ddot{\theta} + I_x p\dot{\psi}\sin\theta - I\dot{\psi}^2\sin\theta\cos\theta \\ M_\zeta &= I(d/dt)(\dot{\psi}\sin\theta) + I\dot{\theta}\dot{\psi}\cos\theta - I_x p\dot{\theta} \end{aligned} \tag{1}$$

where the roll rate p is defined by

$$p = \dot{\phi} + \dot{\psi}\cos\theta \tag{2}$$

The angular rate $\dot{\phi}$ is the windward-meridian rotation rate, i.e., the roll rate with respect to the wind. It is assumed that the aerodynamic moments consist only of pitch or yaw moments from angle of attack, an arbitrary roll moment, and pitch and yaw damping moments. It is further assumed that the vehicle is aerodynamically axisymmetric (i.e., $C_{N_\alpha} = C_{N_\beta}$), so that the restoring torque from angle of attack is independent of the roll orientation ϕ and dependent only on θ. The moments are then written

$$\begin{aligned} M_\xi &= C_l qSd \\ M_\eta &= -C_{N_\alpha} qSl\theta - (qSd^2/2u)[-C_{m_q} + (2C_{N_\alpha} I/md^2)]\dot{\theta} \\ M_\zeta &= -(qSd^2/2u)[-C_{m_q} + (2C_{N_\alpha} I/md^2)]\dot{\psi}\sin\theta \end{aligned} \tag{3}$$

where l is the vehicle static margin (considered positive for the statically stable vehicle), and the damping terms consist of both the pitch (or yaw) damping derivative C_{m_q} and a normal force damping term $2C_{N_\alpha} I/md^2$ to account for lateral motion of the vehicle center of mass.†

Substituting Eq. (3) in Eq. (1) and dividing the second two equations by I and the first by I_x gives

$$\begin{aligned} \kappa &= \dot{p} \\ -\omega^2\theta - \nu\dot{\theta} &= \ddot{\theta} + \mu p\dot{\psi}\sin\theta - \dot{\psi}^2\sin\theta\cos\theta \\ -\nu\dot{\psi}\sin\theta &= d/dt(\dot{\psi}\sin\theta) + \dot{\theta}\dot{\psi}\cos\theta - \mu p\dot{\theta} \end{aligned} \tag{4}$$

where the coefficients are

$$\begin{aligned} \omega^2 &= C_{N_\alpha} qSl/I \qquad \kappa = C_l qSd/I_x \\ \nu &= (qSd^2/2Iu)(-C_{m_q} + 2C_{N_\alpha} I/md^2) \qquad \mu = I_x/I \end{aligned} \tag{5}$$

The parameter ω is the natural pitch frequency of the vehicle.

† It can be shown, for an axisymmetric vehicle, that the lateral motions of the center of mass from normal forces acting at the center of mass are proportional to pitch or yaw rotations about a point a distance I/ml ahead of the center of mass.

III. Quasi-Steady Solution for Angle-of-Attack Convergence

The vehicle motion during re-entry, described in terms of the time-dependent Euler angles $[\psi(t),\phi(t),\theta(t)]$, is assumed to be of the form

$$[\psi(t),\phi(t),\theta(t)] = [\bar{\psi}(t),\bar{\phi}(t),\bar{\theta}(t)] + [\psi_+(t),\phi_+(t),\theta_+(t)] \tag{6}$$

where $[\bar{\psi}(t),\bar{\phi}(t),\bar{\theta}(t)]$ represents a quasi-steady component that varies relatively slowly with time (of the order of the dynamic pressure) and $[\psi_+(t),\phi_+(t),\theta_+(t)]$ represents an oscillation of higher frequency about the average (quasi-steady) values. In the ensuing analysis, the oscillations are neglected and a solution is obtained for the quasi-steady angle-of-attack convergence behavior of the descending vehicle. This development is heuristic in nature and based on physical intuition. It is justified on the basis of agreement with more complete and lengthier analyses presented later.

Taking $\sin\theta \approx \theta$ and $\cos\theta \approx 1$ and neglecting pitch damping ν in the second of Eqs. (4) gives, for the pitch equation

$$\ddot{\theta} + (\omega^2 + \mu p\dot{\psi} - \dot{\psi}^2)\theta = 0 \tag{7}$$

This equation describes a nonlinear oscillation in θ about a nonzero quasi-steady value $\bar{\theta}$, since θ, by definition, is always positive. One can interpret the corresponding quasi-steady values of $\dot{\psi}$ to be those that make $\ddot{\theta}$ in Eq. (7) zero, thus satisfying the relation

$$\omega^2 + \mu p\bar{\dot{\psi}} - \bar{\dot{\psi}}^2 = 0$$

or

$$\bar{\dot{\psi}}_{+,-} = p_r \pm (p_r^2 + \omega^2)^{1/2} \tag{8}$$

where $p_r \equiv \mu p/2$ is a reduced roll rate parameter, and the $+$ and $-$ subscripts designate the positive and negative roots, respectively. This result is valid as long as θ is appreciably greater than the trim angle of attack from aerodynamic or mass asymmetries (assumed to be zero for the present analysis). In the limit $\omega \to 0$ (exoatmospheric), Eq. (8) reduces to the two values $2p_r$, 0. Deeper in the atmosphere, where ω has increased such that $p_r \ll \omega$, $\bar{\dot{\psi}}$ has the approximate values

$$\bar{\dot{\psi}}_+ = \omega + p_r, \quad \bar{\dot{\psi}}_- = -\omega + p_r \tag{9}$$

This indicates that, for values of angle attack sufficiently greater than trim, the precession rate $\dot{\psi}$ can oscillate in either a positive or negative mode, the quasi-steady value of which is slightly displaced from the natural pitch frequency for a slender vehicle.‡ The mode of oscillation depends on the initial re-entry conditions and is discussed later. Once $\dot{\psi}$ is determined, the windward-meridian rotation $\dot{\phi}$, for small θ, is simply the difference between the roll rate p (assumed known) and $\dot{\psi}$.

The angle-of-attack convergence can be obtained from the third of Eqs. (4). This equation can be written

$$(d/dt)(\dot{\psi}\sin^2\theta) + \nu\dot{\psi}\sin^2\theta - \mu p\dot{\theta}\sin\theta = 0 \tag{10}$$

We now consider the time variation of the quasi-steady values $\bar{\theta}$ and $\bar{\dot{\psi}}$ by writing Eq. (10) with assumption of small θ in the form

$$(d/dt)\bar{\theta}^2 + f(t)\bar{\theta}^2 = 0 \tag{11}$$

where

$$f(t) \equiv [(d\bar{\dot{\psi}}/dt) + \nu\bar{\dot{\psi}}]/[\bar{\dot{\psi}} - p_r] \tag{12}$$

‡ The two precession modes, Eqs. (8) or (9), are analogous to the fast and slow precession of a spinning top but differ in sign, because the pitch moment acts in the opposite direction to the top turning moment for a statically stable missile.

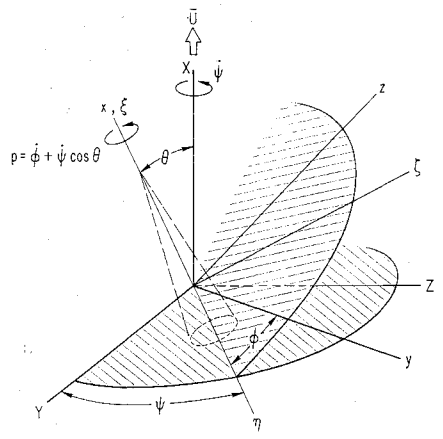

Fig. 1 Euler angles for three-degree-of-freedom rotational motion.

Equation (11) has the familiar solution

$$\left(\frac{\bar{\theta}}{\theta_0}\right)^2 = \exp\left(-\int_0^t f(t')dt'\right) \tag{13}$$

On substituting $\bar{\dot{\psi}}$ from Eq. (8) in Eq. (12) and integrating this result in Eq. (13) we find, for the quasi-steady angle-of-attack convergence, the expression

$$\frac{\bar{\theta}}{\theta_0} = (1+\sigma^2)^{-1/4}\exp\left\{-\frac{1}{2}\int_0^t\left(\frac{\dot{p}}{p}\right) + \nu \times [1 \pm (1+\sigma^2)^{-1/2}]dt\right\} \tag{14}$$

where $\sigma \equiv \omega/p_r$. The plus and minus signs in the exponent correspond to the positive and negative modes, respectively, of the precession rate $\dot{\psi}$. The roll acceleration term $\dot{p}/p$ in the exponent is an effective damping term that adds to or subtracts from the damping coefficient ν, depending on the direction of the roll acceleration.§ Similarly, the term $(1+\sigma^2)^{-1/2}$ either increases or decreases the effective damping and, therefore, increases or decreases the rate of angle-of-attack convergence, depending on whether the precession mode is positive or negative. The conditions that determine the precession mode are discussed later.

For a slender re-entry vehicle, $\mu \ll 1$, the parameter σ^2 is generally much greater than unity except for highly supercritical roll rates $p \gg \omega$. Therefore, in most cases the term $(1+\sigma^2)^{-1/2}$ in the exponent of Eq. (14) can be ignored compared with unity, and Eq. (14), with the assumption $1+\sigma^2 \approx \sigma^2$, reduces to

$$\frac{\bar{\theta}}{\theta_0} = \left(\frac{\mu p_0}{2\omega}\right)^{1/2}\exp\left(-\frac{1}{2}\int_0^t \nu dt\right) \tag{15}$$

For an exponential atmosphere of scale height H, and with a straight-line trajectory of path angle γ, the integral of Eq. (15) can be evaluated and the angle-of-attack convergence ratio reduces to the simple result

$$\bar{\theta}/\theta_0 = (\mu p_0/2\omega)^{1/2}e^{-b\rho} \tag{16}$$

where

$$b = (HSd^2/8I\sin\gamma)(-C_{m_q} + 2C_{N\alpha}I/md^2) \tag{17}$$

and ρ is density. The results, Eq. (15) or (16), indicate that for roll rates that are not excessively supercritical [i.e., for $(1+\sigma^2)^{-1/2} \ll 1$], the angle-of-attack convergence depends only on the re-entry roll rate and is independent of roll acceleration.

§ It appears that negative (decelerating) values of $\dot{p}$ that yield negative values for the effective damping coefficient $[(\dot{p}/p) + \nu]$ would produce a momentary angle-of-attack divergence. Such cases might prove interesting for future investigations.

For the constant roll rate case ($\dot{p} = 0$), the result, Eq. (14), reduces to an expression similar to that derived in Ref. 1 for the negative precession mode.

IV. Initial Re-Entry Conditions

Before re-entry, the vehicle is in a state of moment-free motion, and the relation between the various angular rates is uniquely determined. In general, the vehicle will have some initial roll rate p_0 and will undergo a steady precession (coning motion) with a precession rate Ω and cone half-angle α (Fig. 2a). The cone axis will, in general, be inclined to the flight path, and the velocity vector may lie inside the coning circle (Fig. 2b) or outside the coning circle (Fig. 2a). Special limiting cases of exoatmospheric motion, in which the vehicle is at angle of attack with no coning or is coning symmetrically about the flight path, are shown in Figs. 2c and 2d, respectively. The exoatmospheric roll rate, precession rate, and cone half-angle are related by the expression

$$\Omega = \mu p_0/\cos\alpha \tag{18}$$

This relation follows from the second of Eqs. (4) with $\dot{\theta} = \ddot{\theta} = \omega = 0$, and α and Ω substituted for θ and $\dot{\psi}$, respectively.

After entering the atmosphere, the statically stable vehicle is subjected to an aerodynamic pitch moment that tends to align the vehicle with the flight path. However, because of the angular momentum comprised of the roll and precession rates, which, on the average, is directed along the coning axis, the pitch motion is resisted by gyroscopic forces that induce a precession of the angular momentum vector about the average flight path. This precession is opposite in direction to the angular momentum (retrograde precession) for the cases shown in Figs. 2a and 2c. A projection of the path described by the nose of the vehicle on a plane perpendicular to the flight path would be as shown in Figs. 3a and 3b when the path is viewed along the direction of flight. The residual coning motion, in the same direction as the angular momentum vector (clockwise), has been called nutation by Nicolaides,[7] and the retrograde precession in the opposite direction (counterclockwise) has been called, simply, precession.¶ In general, the two motions exist simultaneously. For the special case of Fig. 3c, in which the vehicle is coning symmetrically about the flight path in the positive direction (direct precession), the pitch moment tends to induce a precession in the opposite direction. This condition is therefore quasi-stable, but it can persist throughout the trajectory. For the case shown in Fig. 2b, in which the coning is initially asymmetric about the velocity vector, an instability can occur in which the motion changes from direct precession to retrograde precession. This is discussed later.

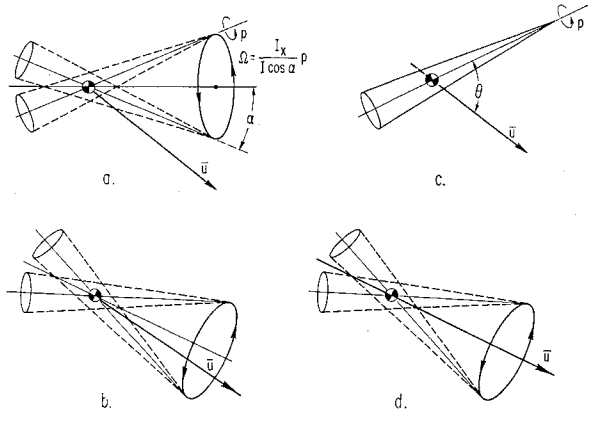

Fig. 2 Possible exoatmospheric motions.

¶ These definitions are more restrictive than are the classical definitions of nutation and precession as being variations in θ and ψ, respectively (see, for example, Ref. 9, p. 432).

The Euler angles ψ, ϕ, θ were defined with respect to an inertial frame of reference that moves along the flight path such that $\dot{\psi}$ represents precession about the velocity vector (Fig. 1). Therefore, the two exoatmospheric conditions represented in Figs. 2c and 2d correspond to initial conditions on $\dot{\psi}$ of $\dot{\psi}_0 = 0$ and $\dot{\psi}_0 = \Omega = \mu p_0/\cos\theta_0$, respectively. Referring back to the quasi-steady solution for $\dot{\bar{\psi}}$, Eq. (8), we note that, in the limit as $\omega \to 0$, corresponding to zero atmospheric density, $\dot{\bar{\psi}}$ can have the two values 0 and μp (the latter value would be $\mu p/\cos\theta$, without the small angle approximations in Eq. 7). Therefore, the two precession modes of Eq. (8) correspond initially to the two cases of exoatmospheric motion shown in Figs. 2c and 2d. This analysis may be related to the epicyclic or tricyclic theories of Nicolaides.[7] The two motions, Figs. 3a and 3c, represent what Nicolaides terms pure "precession" and pure "nutation," respectively. The precession and nutation frequencies of the rotating vectors in Nicolaides' theory are precisely the two precession rates of Eq. (8). However, the development of Eq. (8) reveals that two modes of motion can exist for which the average or quasi-steady value of the precession rate is either the precession or nutation frequency of Nicolaides. Under certain conditions when the initial precession mode is positive, an instability can occur in the presence of roll acceleration whereby the motion changes from the positive to the negative precession mode. A criterion is derived in the next section for predicting this instability.

The expression derived above for angle-of-attack convergence, Eq. (14), corresponds to the two limiting cases, Figs. 3a and 3c. The negative sign in the exponent of Eq. (14) corresponds to the retrograde precession mode and the positive sign corresponds to the direct precession mode.

V. Precession Instability

Equation (10) describes the relation between the total angle of attack θ and the precession rate $\dot{\psi}$, without any assumption of quasi-steady motion. This equation with the assumption of small θ can be written in the form

$$\dot{\theta} = -\{[(d\dot{\psi}/dt) + \nu\dot{\psi}]/2(\dot{\psi} - p_r)\}\theta \tag{19}$$

which reveals much about the vehicle motion. First, we note that θ, by definition, is always positive and $\dot{\psi}$, from these considerations, oscillates about either the positive or the negative branch of the natural pitch frequency curve ω, as indicated by Eq. (9). Therefore, for $\dot{\psi} > p_r$, the denominator of Eq. (19) remains positive, and, for small damping, $d\theta/dt = 0$ at approximately $d\dot{\psi}/dt = 0$, so that θ and $\dot{\psi}$ oscillate at the same frequency with the θ maxima corresponding to the $\dot{\psi}$ minima and vice versa. Similarly, for $\dot{\psi} < p_r$, the maxima and minima of both θ and $\dot{\psi}$ are in phase. These results can be deduced in another manner. Equation (10), with the assumptions $\nu = 0$ and $\sin\theta \approx \theta$, can be written in the form

$$(d/dt)(\dot{\psi}\theta^2) - p_r(d/dt)(\theta^2) = 0 \tag{20}$$

With the further assumption that p is constant (or slowly varying relative to the θ or $\dot{\psi}$ oscillations), Eq. (20) can be integrated to give

$$(\dot{\psi} - p_r)\theta^2 = \text{const} \tag{21}$$

Equation (21), being the first integral of an equation of motion, is an energy expression and indicates that $|\dot{\psi} - p_r|$ is maximum for θ minimum and vice versa. However, if $\dot{\psi}$ is in the positive mode such that $\dot{\psi} > p_r$, and p increases because of an applied roll torque, an instability will occur as p_r approaches the minimum value of the $\dot{\psi}$ oscillation, which causes the denominator of Eq. (19) to approach zero. It is shown from a phase plane analysis, which follows, that at the point of instability the $\dot{\psi}$ oscillation diverges without limit and finally reverses sign from an infinitely large positive upper bound to an infinitely large negative lower bound.

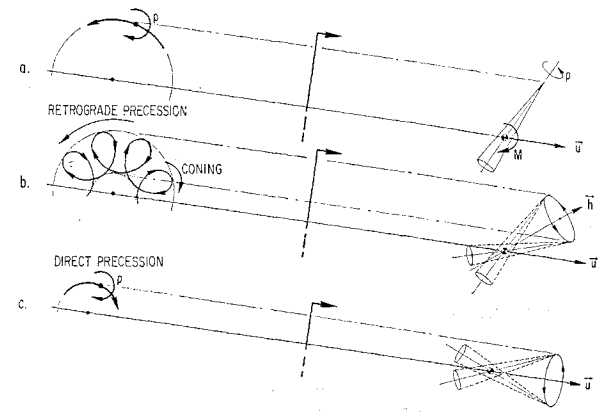

Fig. 3 Precession modes.

Thereafter, $\dot{\psi}$ remains in the more stable negative mode. The divergence in $\dot{\psi}$ corresponds to a lower bound on the θ oscillation that approaches zero, from Eq. (21).

Equations (7) and (19) can be combined to give a single equation in $\dot{\psi}$

$$2(\dot{\psi} - p_r)\left(\frac{d^2\dot{\psi}}{dt^2} + \nu\frac{d\dot{\psi}}{dt} + \dot{\nu}\dot{\psi}\right) - 3\left(\frac{d\dot{\psi}}{dt}\right)^2 + (\mu\dot{p} - 4\nu\dot{\psi}) \times$$

$$\frac{d\dot{\psi}}{dt} + \mu\nu\dot{p}\dot{\psi} - \nu^2\dot{\psi}^2 = 4(\dot{\psi} - p_r)^2(\omega^2 + \mu p\dot{\psi} - \dot{\psi}^2) \tag{22}$$

We can put this equation in a form suitable for phase plane analysis by making the substitutions

$$\begin{aligned} y &\equiv \dot{\psi} - p_r \\ v &\equiv \dot{y} = d\dot{\psi}/dt - \mu\dot{p}/2 \\ vdv/dy &= \ddot{y} = d^2\dot{\psi}/dt^2 \end{aligned} \tag{23}$$

in which $\ddot{p}$ has been assumed to be negligible. Equation (22) is then written

$$\frac{dv}{dy} = \frac{-2y^2(y^2 - a^2) + cy(y + d) + \frac{3}{2}v(v + b) + \nu vy}{yv} \tag{24}$$

where

$$\begin{aligned} a &\equiv (\omega^2 + p_r^2)^{1/2},\ b \equiv \tfrac{2}{3}\mu(\dot{p} + \nu p) \\ c &\equiv \tfrac{1}{2}(\nu^2 - 2\dot{\nu}),\ d \equiv \mu p(\nu^2 - \dot{\nu})/(\nu^2 - 2\dot{\nu}) \end{aligned} \tag{25}$$

The parameters, a, b, c, d, and ν vary slowly with time (of the order of the dynamic pressure) relative to y and are assumed to be constants in the ensuing analysis. The stability conditions so obtained from a phase plane evaluation of Eq. (24) apply at any instant of time with the appropriate values of these parameters. However, since these parameters do change with time, the nature of the motion and the stability criteria change accordingly. This is discussed in greater detail later.

Singularities in the $v - y$ plane [points where the right side of Eq. (24) takes the form zero over zero] are seen to occur at

$$\begin{aligned} y &= 0,\ v = 0 \\ y &= 0,\ v = -b \\ y &= y_1,\ v = 0 \\ y &= y_2,\ v = 0 \\ y &= y_3,\ v = 0 \end{aligned}$$

where y_1, y_2, and y_3 are roots of

$$y^3 - [a^2 + (c/2)]y - cd/2 = 0 \tag{26}$$

Since c and d are, in general, much smaller than a^2, these roots

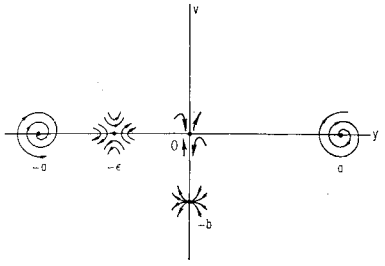

Fig. 4 Singularities in phase plane.

are approximately

$$y_1 \approx a,\ y_2 \approx -a,\ y_3 \approx -\epsilon \tag{27}$$

where $\epsilon \approx -cd/2a^2$. We now examine the character of the singularities in order to construct the solution curves to the equations of motion.

By a suitable transformation of coordinates with the origin shifted to the singularity, all of the singularities except that at $y = 0, v = 0$ can be reduced to a form governed by the differential equation

$$dv/dy = (Ay + Bv)/(Cy + Dv) \tag{28}$$

The nature of the singularity depends on the relative magnitudes of the constants A, B, C, and D and the various special cases of Eq. (28) have been characterized.[10] The four singularities governed by Eq. (28) are summarized in Table 1.

The singularities at $\pm a$, 0 signify the existence of either stable or quasi-stable oscillations in y about the equilibrium values $y = \pm a$, depending on the magnitude of pitch damping and roll acceleration. Moreover, the oscillations about $y = +a$ are of either constant or diverging amplitude, corresponding to the center or unstable spiral singularities, whereas the oscillations about $y = -a$ may be either of constant, diverging, or converging amplitude, depending on the relative magnitudes of the pitch damping and roll acceleration. From the definition of y, Eq. (23), the oscillations in y about $\pm a$ correspond to the direct and retrograde precession oscillations in $\dot{\psi}$ about the positive and negative branches, respectively, of the natural pitch frequency curves.

The aforementioned considerations are based on the assumption of quasi-steady motion for which the parameters defined by Eq. (25) were assumed to be constants. However, since these parameters change slowly with time, they influence the character of the motion. Consider, for example, the oscillation in y about the singularity $y = +a$ and let there be a positive roll acceleration so that the roll rate p increases with time. The increase in p reduces y, whereas the value a about which y oscillates increases approximately as the natural pitch frequency. The net effect is to increase the amplitude of the oscillation; this increase is characteristic of the unstable spiral singularity that exists at $y = +a$ with the presence of a roll acceleration. It will be shown that if p increases sufficiently to drive y to zero (i.e., p_r approaches

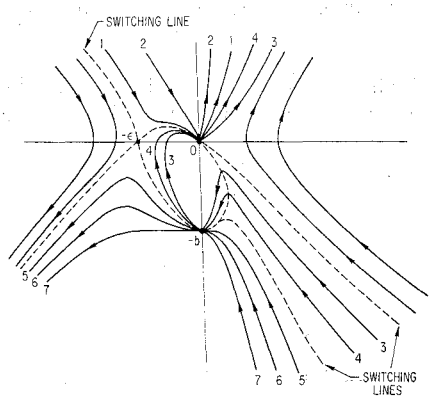

Fig. 5 Solution curves in neighborhood of origin.

Table 1 Character of singularities

Singularity	Type
$y = a, v = 0$	unstable spiral; center for $\nu = \dot{p} = 0$
$y = -a, v = 0$	stable or unstable spiral depending on ν and $\dot{p}$; center for $\nu = \dot{p} = 0$
$y = 0, v = -b$	unstable node
$y = -\epsilon, v = 0$	saddle

the minimum value of $\dot{\psi}$), an instability occurs whereby the motion reverses from an oscillation about $y = +a$ to a more stable oscillation about $y = -a$. The nature of the crossover becomes apparent from the character of the singularities near the origin.

The singularity at the origin, $y = 0, v = 0$, is a higher-order singularity than those characterized by Eq. (28), and the nature of the singularity is not readily determined analytically. Consequently, a numerical technique such as the method of isoclines[11] is required for determining the behavior of the solution curves in the neighborhood of the singularity. Figure 4 summarizes, schematically, the character of the four singularities summarized in Table 1 plus the higher-order singularity at the origin deduced from limiting cases of Eq. (24). The relative spacing between the singularities is grossly distorted, since ϵ is, in general, a very small quantity compared with a. The qualitative behavior of the solution curves in the neighborhood of the singularities near the origin, as determined from a plot of Eq. (24) by the method of isoclines, is shown in Fig. 5. The nature of the crossover from an oscillation about the positive branch of the pitch frequency curve to an oscillation about the negative branch now becomes apparent. Figure 5 shows that there are two switching lines in the positive halfplane and one in the negative halfplane. To the right of the first switching line, an oscillation about the positive branch persists until the amplitude reaches sufficient magnitude to reach the first switching line as $y \to 0$. It then appears possible to follow a trajectory between the two switching lines that will pass through the singularities but continue around the positive branch (trajectories labeled 3 and 4). Beyond the second switching line the trajectory loops around the negative branch ($y = -a$) and can return to the positive branch provided it passes to the right of the switching line in the negative halfplane (trajectories 1 and 2). This motion through the singularities at the origin represents a brief period of instability, which occurs only at the instant $y \to 0$. In view of the decreasing value of y due to the increase in roll rate, it would be expected that only a small number of trajectories, if any, would pass through this region. To the left of the origin, as y continues to decrease due to the increasing roll rate, the oscillations appear to become more stable about the negative branch, as represented by the trajectories to the left of the singularity at $-\epsilon$. This behavior has been verified by computer solutions of the equations of motion, which are discussed later.

Some further insight can be obtained from a physical interpretation of the relation, Eq. (19), between the angle of attack and the precession rate. From the definition for y, Eq. (23), the limiting case $y = 0$ corresponds to a zero value of the denominator on the right side of Eq. (19). But since

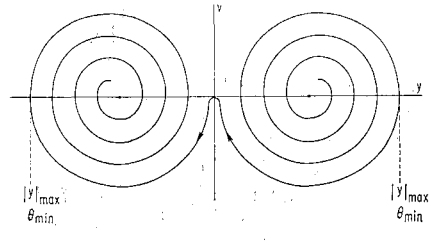

Fig. 6 Qualitative behavior of solution curves in phase plane.

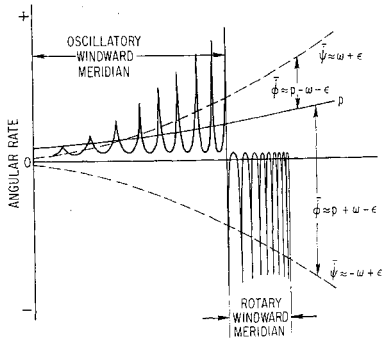

Fig. 7 Windward meridian behavior.

θ, by definition, is always positive, this would represent an instability in θ (i.e., a large value of $\dot{\theta}$) unless either θ or $(d\dot{\psi}/dt) + \nu\dot{\psi}$ also approached zero along with y. What is found from the computer solutions is that θ does approach zero in the region of instability, since the θ oscillations are coupled with the $\dot{\psi}$ oscillations through Eq. (21). From conservation of energy, as θ approaches its minimum $|\dot{\psi} - p_r|$ approaches its maximum and vice versa. Therefore, the extreme values of $\dot{\psi}$(or y), both positive and negative, will occur in the region of instability as $y \to 0$. This is shown qualitatively in Fig. 6.

The foregoing discussion has dealt with the precession rate $\dot{\psi}$, which is related to the roll rate p and the windward-meridian rotation rate $\dot{\phi}$ through Eq. (2). For small θ, this relation is approximately

$$p \approx \dot{\phi} + \dot{\psi} \tag{29}$$

From the first of Eqs. (4), the roll rate is gyroscopically uncoupled from the other angular rates and depends only on the roll moment coefficient. Therefore, for a prescribed roll history, the windward-meridian rotation rate is simply the difference $\dot{\phi} = p - \dot{\psi}$. Depending on the roll history and on whether $\dot{\psi}$ is in the positive or negative mode, the windward meridian may be either "oscillatory" or "rotary"; i.e., the vehicle either oscillates about its roll axis relative to the wind or rotates continuously in one direction. This is illustrated in Fig. 7 for an arbitrary roll rate history. When $\dot{\psi}$ is in the positive mode with the roll history shown, $\dot{\phi}$ oscillates from positive to negative with the quasi-steady value $\bar{\dot{\phi}} \approx p - \omega$. However, for $\dot{\psi}$ in the negative mode, $\dot{\phi}$ does not change sign, and the windward meridian therefore rotates continuously in one direction. Since, as shown above, the negative $\dot{\psi}$ mode is more stable, the windward meridian is more likely to be rotary, but either mode may persist, depending on the roll history.

VI. Computer Solutions

Figures 8 and 9 show computer solutions of the equations of motion [Eqs. (4)] for the angle of attack and angular rates corresponding to the two limiting cases of exoatmospheric motion shown in Figs. 2c and 2d. Also shown for comparison with the computer results are quasi-steady approximations for the angle-of-attack convergence, calculated from Eq. (14).

Since the precession rate $\dot{\psi}$ is initially zero for the case of Fig. 8, and $\dot{\psi} = 0 < p_r$, the vehicle will precess in the negative mode following re-entry and will remain in the negative mode until the angle of attack approaches trim. This is verified from the computer result. Alternatively, for the case of Fig. 9, $\dot{\psi}$ is initially positive and greater than the reduced frequency p_r. Therefore, $\dot{\psi}$ continues to precess in the positive mode and remains positive as long as the minimum value of the oscillation envelope remains greater than p_r. The reduced frequency is also plotted in Fig. 9 and remains less than the minimum value of $\dot{\psi}$ throughout the trajectory. Consequently, $\dot{\psi}$ remains in the positive mode, as verified by the computer result. The windward meridian remains rotary in this case, since the oscillation in $\dot{\psi}$ is small enough that the difference $p - \dot{\psi}$ remains positive.

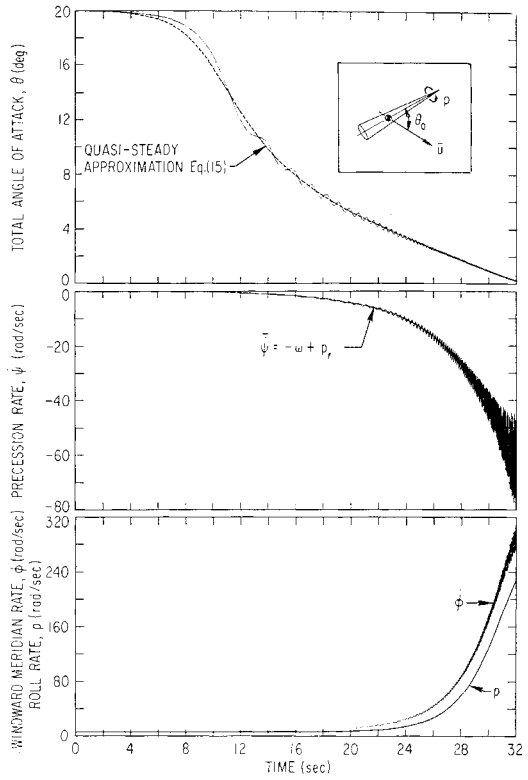

Fig. 8 Motion history for nonprecessing vehicle at re-entry.

Figure 10 corresponds to a re-entry in which the vehicle is coning initially about an axis inclined to the flight path. The precession rate $\dot{\psi}$ with respect to the flight path is positive initially and oscillates with an upper and lower bound. The lower bound is plotted against the reduced roll rate in Fig. 11 and is greater than p_r initially. However, the roll

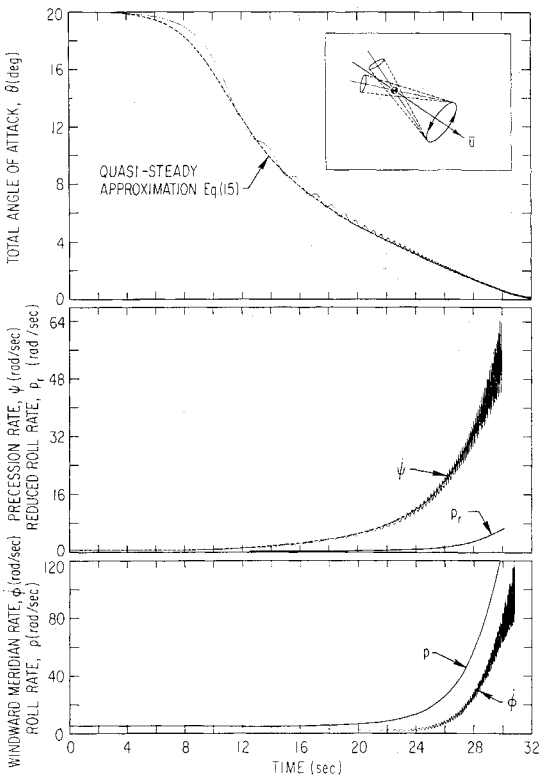

Fig. 9 Motion history for symmetric precession about flight path at re-entry.

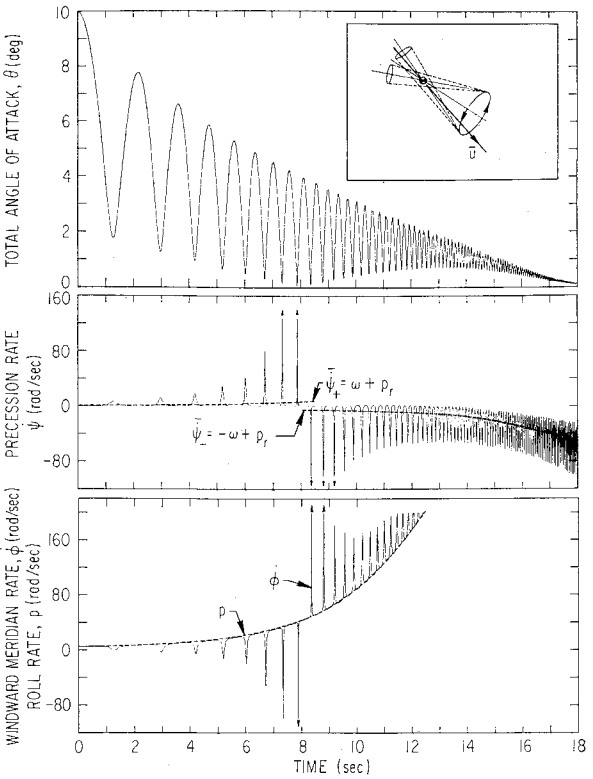

Fig. 10 Motion history for unsymmetric precession about flight path at re-entry.

rate increases because of an applied roll torque, and the reduced roll rate approaches the minimum value of $\dot{\psi}$ after approximately 8 sec, which causes $\dot{\psi}$ to become unstable. Simultaneously, the lower bound of the angle-of-attack oscillation envelope approaches zero as the upper bound of $\dot{\psi}$ diverges, and $\dot{\psi}$ reverts to the more stable negative mode. The character of the motion also changes after the instability, as shown in Fig. 12, which is a polar plot of the angle of attack versus the precession angle ψ. Before the instability, the motion is characterized by "flower petal" loops containing the origin, whereas after the instability, the loops do not contain the origin (retrograde precession).

VII. Summary and Conclusions

A simple expression has been derived for the angle-of-attack convergence of a rolling re-entry vehicle subject to roll acceleration and including pitch and yaw damping. The analytical result has been shown to compare favorably with computer solutions of the equations of motion. The effect of roll acceleration on the angle-of-attack convergence envelope is identical to the effect of pitch or yaw damping in

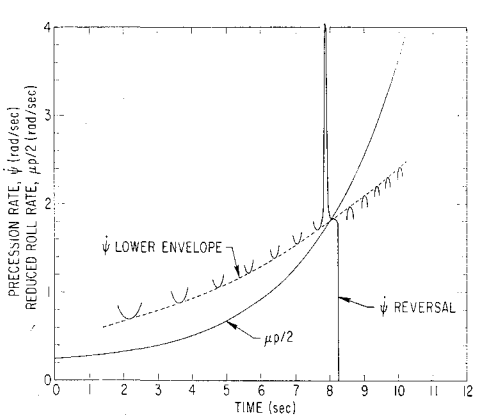

Fig. 11 Precession instability.

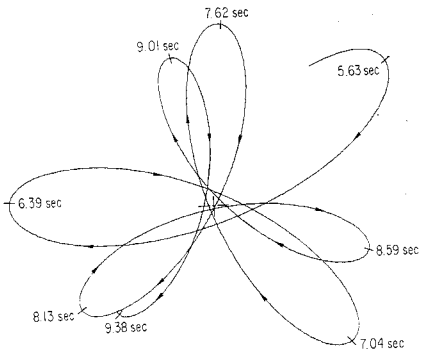

Fig. 12 Polar plot of angle of attack before and after precession instability.

the term $\dot{p}/p$, which either adds to or subtracts from the damping coefficient, depending on the direction of the roll acceleration. The cumulative effects of damping and roll acceleration on the convergence envelope can be significant in certain cases. The angle-of-attack convergence also depends slightly on the mode of precession motion, which depends, in turn, on the initial re-entry conditions.

It has been shown that a rolling re-entry vehicle has two modes of precession motion, either of which can persist, depending on the initial re-entry conditions and on the roll history. The positive mode is quasi-stable and will persist as long as the lower envelope of the precession rate oscillation ($\dot{\psi}$) is greater than the reduced roll rate parameter p_r. If this parameter increases because of roll acceleration until it reaches the lower envelope of the $\dot{\psi}$ oscillation, a precession instability will occur, and the precession rate will change from the positive mode to the more stable negative mode. At the point of instability, the lower envelope of the angle-of-attack oscillation reaches zero. Following the instability, the angle of attack increases slightly, depending on the magnitude of the roll acceleration and on the pitch and yaw damping. The character of a polar plot of angle of attack vs precession angle also changes from "flower petal" loops containing the origin, before the instability (direct precession), to loops that do not contain the origin, after the instability (retrograde precession).

References

[1] Garber, T. B., "On the Rotational Motion of a Body Reentering the Atmosphere," *Journal of the Aerospace Sciences*, Vol. 26, No. 7, July 1959, pp. 443–449.

[2] Leon, H. I., "Angle of Attack Convergence of a Spinning Missile Descending Through the Atmosphere," *Journal of the Aerospace Sciences*, Vol. 25, No. 8, Aug. 1958, pp. 480–484.

[3] Tobak, M. and Peterson, V. L., "Angle-of-Attack Convergence of Spinning Bodies Entering Planetary Atmospheres at Large Inclinations to the Flight Path," TR R-210, Oct. 1964, NASA.

[4] Longmire, C. L., "Reentry of Rotating Missiles," Research Note 213, Dec. 1960, Avco Everett Research Lab., Avco Corp., Everett, Mass.

[5] Albini, F. A., "Oscillation Envelope for a Spinning Reentry Vehicle," Rept. 21838, Feb. 27, 1962, Hughes Aircraft Co., Space Systems Division, El Segundo, Calif.

[6] McShane, E. G., Kelley, J. L., and Reno, F. V., *Exterior Ballistics*, Univ. of Denver Press, Denver, Colo., 1953.

[7] Nicolaides, J. D., "On the Free Flight Motion of Missiles Having Slight Configurational Asymmetries," Rept. BRL-858, June 1953, Ballistic Research Labs., Aberdeen Proving Ground, Md.

[8] Thomson, W. T., *Introduction to Space Dynamics*, Wiley, New York, 1961.

[9] Synge, J. L. and Griffith, B. A., *Principles of Mechanics*, 2nd ed., McGraw-Hill, New York, 1949.

[10] Stoker, J. J., *Nonlinear Vibrations in Mechanical and Electrical Systems*, Interscience, New York, 1950.

[11] DeRusso, P. M. et al., *State Variables for Engineers*, Wiley, New York, 1965.